

CARROLL COLLEGE

A Look into Railgun Physics and Design

Senior Honors Thesis

Scott Harmon

April 2011

Railguns promise to make space travel and weapons systems much more efficient for the future. I conducted a project to skim the surface of railgun physics and design. I first started by constructing a small railgun as a proof-of-concept. I then delved deeper into the physics of operation by measuring and modeling the magnetic field associated with the operation of the device.

The model railgun had all of the basic components of much larger, more complicated devices. It consisted of a pair of rails, a bank of powerful capacitors, a charging circuit, and an AC power source. When the capacitors were charged to 60 volts, I estimated the force on the projectile to be 9.12×10^{-6} Newtons. Unfortunately, this was not enough force to overcome friction forces as well as tertiary “welding” of the projectile to the rails.

In order to understand the basic physics principles behind the operation of the railgun, I measured the magnetic field produced by the rails. The field produced by a single rail was very non-uniform, revealing weaknesses in my initial rail design. I then conducted the same experiment, but with a solid wire. This produced the expected magnetic field, which was relatively small on the ends, with the maximum in the center of the length of wire. This taught me that a solid wire produces a desirable magnetic field, rather than my initial design that had many air-filled voids within the rails.

With the knowledge gleaned from this immersion into railgun physics, I will be able to better design similar devices in the future with a greater understanding of magnetic field production.

Contents

| | |
|--|----|
| Table of Figures | 4 |
| Introduction..... | 5 |
| Principle of Operation | 8 |
| Physics of Operation..... | 11 |
| Physical Model..... | 13 |
| Basic Design..... | 13 |
| Loading and Firing the Projectile..... | 15 |
| Consequences of the Design | 16 |
| Safety Issues | 17 |
| Model Results..... | 20 |
| Data Analysis | 22 |
| Consequent Investigation..... | 25 |
| Conclusion and Future Work..... | 28 |
| Appendix A | 29 |
| Appendix B..... | 30 |
| Appendix C..... | 31 |
| Works Cited | 32 |

Table of Figures

| | |
|---|----|
| <i>Figure 1: Diagram of railgun principle of operation (Harris, 2005).</i> | 8 |
| <i>Figure 2: The railgun model. The VariAC and polypipe launch tube are to the left of the device itself.</i> | 13 |
| <i>Figure 3: Railgun charge/discharge circuit</i> | 14 |
| <i>Figure 4: Pictured is the capacitor bank, with the copper strips which form the electrical connection visible. Contact with these strips when the capacitors is a significant safety risk.</i> | 18 |
| <i>Figure 5: The exposed charging circuit, illustrating the potential danger of this component. All visible electrical connections carry charging voltage, which is generally between 10 and 120 volts.</i> | 19 |
| <i>Figure 6: Long exposure of railgun test-fire at 60 volts. The orange, arcing streak is the trajectory of the ball. Note the tube used to impart initial velocity to the ball in order to prevent sticking.</i> | 20 |
| <i>Figure 7: Distance from left end of rail vs. current-normalized magnetic field. The second data point is missing due to construction limitations.</i> | 22 |
| <i>Figure 8: Distance from left end of rail vs. current-normalized magnetic field. Note the smooth curve, which is expected for this experiment.</i> | 24 |
| <i>Figure 9: Numerical method for calculating magnetic field from a finite wire.</i> | 26 |
| <i>Figure 10: Numerical approximation of magnetic field data in red, with actual data plotted in blue. This data replicates that of the single wire measurement experiment.</i> | 26 |
| <i>Figure 11: A comparison of magnetic field measurement, numerical approximation, and Ampere's Law. The numerical model is at least 60% better than Ampere's law at approximating the measured data.</i> | 29 |

Introduction

Railguns use very basic laws of electromagnetic theory to propel an object. A large current is used to generate a magnetic field, which accelerates the projectile to a high speed. The first railgun was designed by Louis Octave Fauchon-Villeplee in 1918 (Fauchon-Villeplee, 1922). The first practical application for railguns was realized during World War II, when the German Luftwaffe Flak Command issued a specification for a railgun-based anti-aircraft weapon. It was never built, but the discovery of the plans by Allies after the war sparked further interest in railgun-based weapons (Hogg, 1969). Interest in railguns today is not limited to military uses, but also includes launching satellites and other commercial applications.

Railguns have several advantages over chemical propellant-based weapons. The first and most important is the increase in theoretical muzzle velocity and range. The 16" Mark 7 gun used on Iowa-class battleships during World War II had a maximum range of over twenty-three miles using 1,900-pound projectiles (NavWeaps, 2009). The Mark 7 is one of the most powerful guns ever used extensively in service, but pales in comparison to the theoretical ability of a railgun. Railguns, however, do not have these limitations. Since the force on the projectile is proportional to the current applied, there is no theoretical limit to the amount of force applied to the projectile. This means the maximum range and velocity are without theoretical limit. Of course, due to the presence of atmosphere, gravity, friction, and other forces, limitless force is impossible. However, railguns still have the ability to fire projectiles faster and farther than conventional powder weapons. Also, more ammunition can be stored in a given space, due to the fact that railguns do not use chemical propellant. Another advantage is that due to the extreme velocities developed, explosive shells are not necessary. The shells carry enough kinetic energy to destroy even hardened targets without the help of explosives. This makes the storage

of munitions much safer, as well as eliminating “duds”. The shells are merely slugs of metal, which also have an effectively infinite shelf life.

Railguns have several disadvantages, however. Due to the large electrical currents required, railguns produce huge quantities of heat. This heat increases friction and has the capacity to destroy vital components. Currently, heat is the main hindrance to railgun technology advancement. Powder weapons are much more portable, as each projectile carries its own propellant. Railguns, on the other hand, require large quantities of electricity, which relegates the weapons to permanent use on ships or emplacements on land. Furthermore, powder-based weapons can be fired and cycled much faster, because there is no analogue to the “recharge time” associated with recharging the capacitors necessary to fire a railgun.

I investigated the operation of a railgun by constructing a table-top model. This enabled me to further develop my understanding of the basic physics principles of railgun theory as well as some of the more practical and problematic issues of the operation. The electromagnetic theory of the railgun can be found in introductory physics textbooks, but a deeper study of the railgun reveals the problems that develop due to the large electrical currents involved.

The physical railgun was used to determine the parameters or “dials” that exist for tweaking a railgun’s performance. This helped me to understand more intuitively the inherent strengths and weaknesses of railguns in general, and how to improve the railgun that I built.

One source of inspiration for this project was the website of a group of MIT students (Walter, 1999). They built a similarly-sized railgun using similarly-sized capacitors. Their final design was reminiscent of my current railgun design, with one important difference. They included a spring-assisted compressed air injection system, which launched the projectile at high speed into the railgun, thus imparting significant acceleration. The purpose of the injection system, I believe, is to overcome a problem that I quickly discovered during tests. The lead ball

would readily “stick” to the rails due to the strong electric arcing present during firing. The contact points reached sufficient temperature to melt both the lead and the copper, thus welding the projectile to the rails. This welding, of course, impedes forward motion of the projectile.

Principle of Operation

A railgun is a device which uses electrical current to take advantage of Laplace forces and the Biot-Savart law in order to launch a projectile. The following illustration shows the physics behind railgun operation.

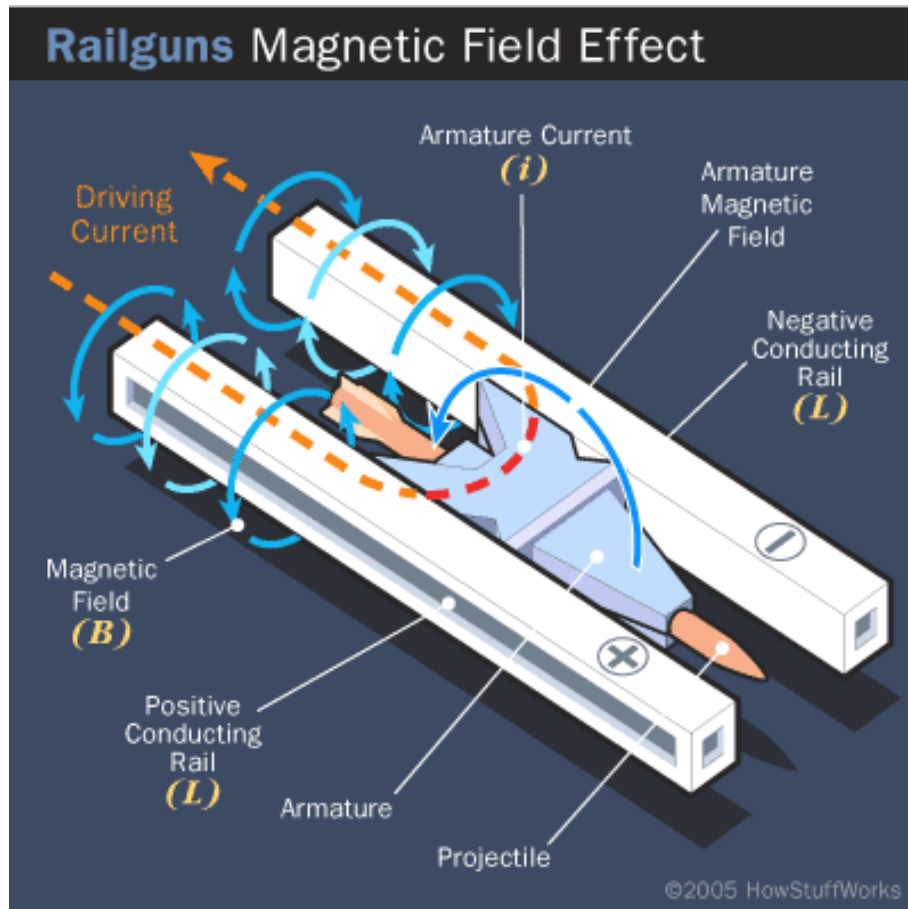


Figure 1: Diagram of railgun principle of operation (Harris, 2005). While this is a good representation of a railgun, the magnetic field around the armature actually goes in the opposite direction.

The magnetic field is produced by the current running through the rails and armature. The current i produces magnetic field \vec{B} in accordance with the Biot-Savart Law, which says that current flowing through a wire will generate a magnetic field proportional to the current magnitude and inversely proportional to the distance from the wire.

The following modified form of the Biot-Savart law can be used to calculate the average magnetic field between the rails during firing (Knight, 2004):

$$B = \frac{\mu_0 I}{2\pi d} \ln\left(\frac{d-r}{r}\right) \quad \text{Eq. 1}$$

μ is the magnetic permittivity constant, I is the current in the firing circuit, d is the rail separation, and r is the radius of the rails. It is important to note that while magnetic fields are vector quantities, this formula yields only the magnitude. The direction of the field must be determined by inspection using the right hand rule. I was concerned with the exact magnetic field at various points along the length of the rails, and as such I did not use this equation. However, it is valuable because it shows how the magnetic field can vary with respect to r and d .

If a current-carrying wire or object is placed in a magnetic field, then that wire or object experiences a force. For the railgun, the object is the armature or projectile seen in Figure One. This force is referred to as the Laplace force and is described by the following equation (Knight, 2004):

$$\vec{F} = i\vec{W} \times \vec{B} \quad \text{Eq. 2}$$

where \vec{F} is the force on the projectile, \vec{B} is the magnetic field vector, \vec{W} is the width vector of the armature, and i is the current in the wire (the length vector is in the direction of current flow). This means that the force on the projectile is proportional to the size of the current, the width of the armature, and the magnitude of the magnetic field (assuming \vec{W} and \vec{B} are perpendicular).

It is important to note that the current through the wire is producing the magnetic field described above, and is also the current-carrying wire referred to by the Laplace force equation

(Eq. 1). Thus, combining this with the equation for Laplace forces, we come to the conclusion that the larger the current, the more force is applied to the projectile. Therefore, a large current is required to fire the projectile at great speed.

Physics of Operation

This project rests (and relies) on work done by Hendrik Lorentz, who first derived the modern-day formula for force due to a magnetic field (Knight, 2004). He developed the formula for Lorentz Forces, shown in Eq. 2 (Knight, 2004):

$$\vec{F} = q[\vec{E} + (\vec{v} \times \vec{B})] \quad \text{Eq. 3}$$

\vec{F} is the force on the point charge q , \vec{E} is the induced electric field vector, \vec{v} is the point charge velocity vector, and \vec{B} is the magnetic field vector. Lorentz forces also manifest themselves in the form of Laplace forces when the magnetic force component is the force acting on a current-carrying wire in a magnetic field. In this situation, the formula becomes:

$$\vec{F} = i\vec{L} \times \vec{B} \quad \text{Eq. 4}$$

\vec{L} is the length vector of the wire, and i is the current in the wire (moving in the direction of the length vector). In the case of the railgun, the electric field is irrelevant. Thus, the $q\vec{E}$ term can be neglected. This is the most useful interpretation of Lorentz forces. Laplace forces are used in many devices, such as loudspeakers, electric motors, and railguns. Lorentz forces are used in less-familiar devices, such as circular particle accelerators, mass spectrometers, and magnetrons (Knight, 2004).

From the perspective of the projectile, the magnetic field produced by the rails is an external field. Thus, the force on the projectile emanates from the magnetic field produced by the rails in accordance with the Biot-Savart Law.

From the perspective of the rails, the current which is passing through them is producing a magnetic field. Since this field cannot act on the object that produces it, they experience no force other than from each other. Clearly, due the Biot-Savart relation, this magnetic field depends on the magnitude of the current through the rails, as well as the resistance of the rails themselves. Theoretically, this magnetic field should form a parabolic shape extending from the rods, with a maximum strength in the center of the length of the rails.

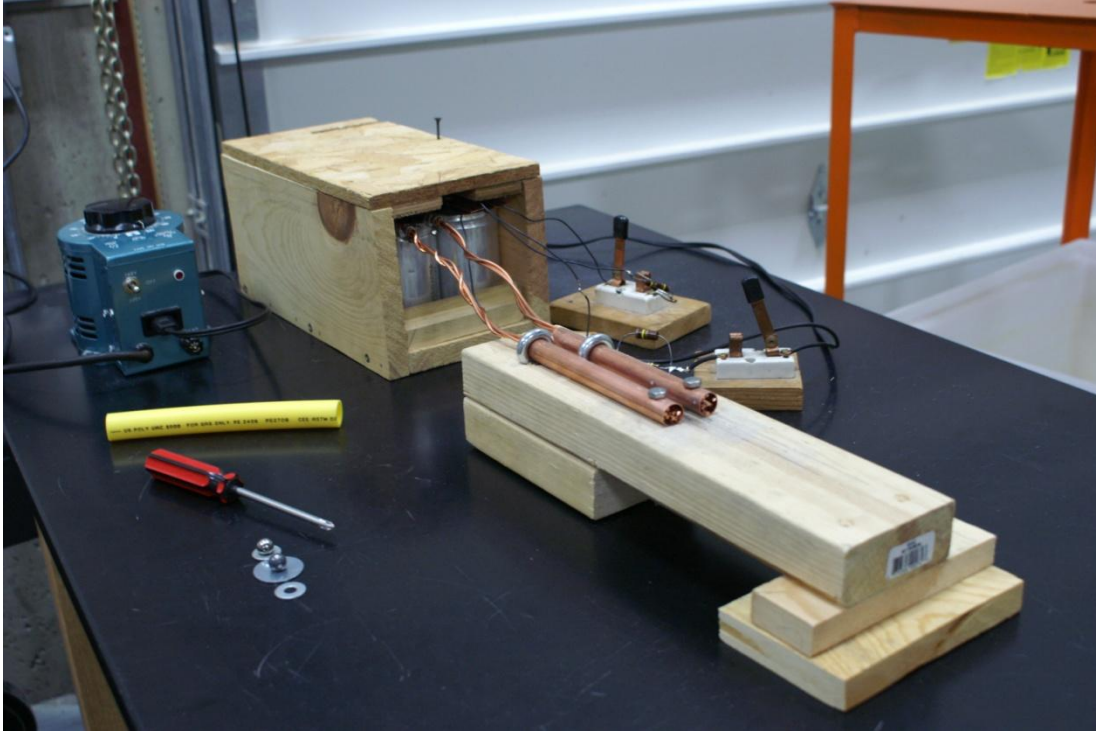


Figure 2: The railgun model. The VariAC and polypipe launch tube are to the left of the device itself.

Physical Model

Basic Design

The railgun model I designed consists of three parts. In the photo shown in figure two, the reader can see the capacitor bank housed in the wooden box. The rails that the projectile travels on are copper water pipe mounted on a wooden base.

The main objective when designing a railgun discharging circuit is to be able to safely produce a large current when firing. This current could be produced in a number of ways, but the most convenient way is using a bank of large capacitors. Capacitors have the advantage of being relatively compact, easy to “arm”, and easy to discharge. Additionally, capacitors can be exposed to a short-circuit situation without risking damage, unlike a battery.

The firing circuit consists of heavy copper strips attached directly to the railgun rails. The two parallel rails were spaced one quarter-inch apart, consisting of one quarter-inch copper water pipe packed with large copper multi-strand wire. The rails were six inches long and bolted to a two-by-four for stability. The rails need to be rigid to prevent the rails from moving apart due to strong repulsive forces during firing. To trigger the device, one needs merely to bridge the two rails with a conductive object, such as ball bearing.

My railgun model uses eight large 350 V, 1.8 mF capacitors in parallel to feed the firing circuit. Together, the maximum amount of energy available is 882 joules. This is enough to theoretically propel a .45 caliber, 133 grain lead ball to approximately 452 m/s (calculations shown in Appendix C). This is about 1,500 ft/s, which is well above the velocity that many powder-based weapons can achieve.

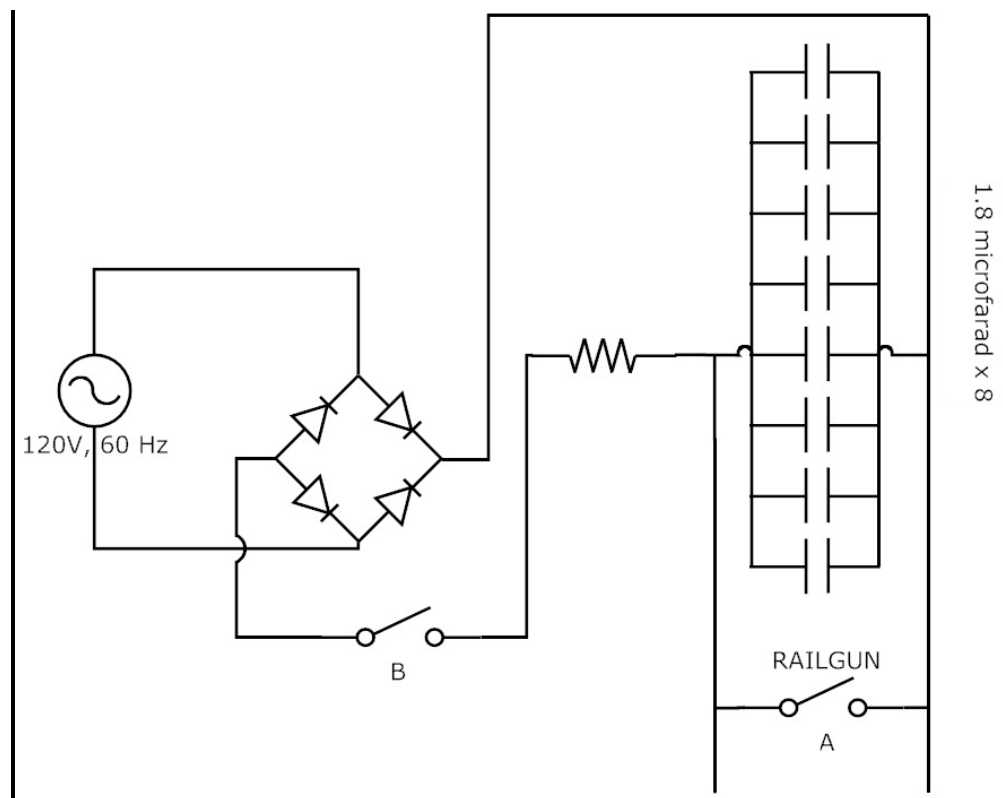


Figure 3: Railgun charge/discharge circuit

Using capacitors means that the railgun circuit must have a way of charging the capacitors. For this design, the power source is essentially line voltage, which is alternating current. Most capacitors require direct current for charging, and so an AC to DC rectifier must be integrated into the circuit. Optionally, there can be a switch in this circuit to prevent current from overloading the diodes in the rectifier and flowing backwards when firing. Finally, a power resistor is required in the charging portion of the circuit to limit current for safety.

Loading and Firing the Projectile

In order to operate the railgun, there needs to be some way to charge and discharge the capacitors. To accomplish this, I designed and built the charging/discharging circuit shown in Figure 3.

This circuit is simple, but works very well to charge and discharge the railgun. The design includes a rectifier of the four diode bridge variety, which was then connected to a resistor (Horowitz, 1980). The purpose of the resistor is to place load on the charging circuit to reduce the current (in accordance with Ohm's Law) to a relatively safe level, and so the value of the resistors can be adjusted to vary the current during charging. A circuit such as this has a characteristic time constant which increases as either the capacitance or the overall resistance increases. Reducing the current in the charging circuit means that it takes longer to charge the capacitors. Additionally, there is a switch in the charging circuit as an additional safety feature, between the rectifier and the resistors, to prevent a back surge of current during firing. The firing circuit is represented by two wires and a switch, where switch B is actually the projectile which would be placed on the rails to activate the device.

To charge the capacitors, switch A is closed while switch B remains open. Physically this means that a projectile is not in the device. The voltage across the capacitors is measured, and

when it reaches the desired voltage, switch A is opened. To fire the railgun, the projectile is placed on the rails, discharging the capacitors. Figure 3 models this as switch B closing.

Consequences of the Design

Unfortunately, there are several problems associated with producing a large current. To handle this massive surge of current, the components of the railgun “downstream” of the capacitors (between the rails and the capacitors) was chosen to minimize resistance while maximizing current-handling capabilities. By this I mean the components must have a high enough heat conductance to prevent excessive local heating which would destroy the device and pose safety problems, while having a large enough mass to prevent the overall device reaching a dangerous temperature. During testing, I discovered that this high current has the ability to “weld” a lead projectile to the copper rails very easily, due to local heating. To mitigate this heat buildup, it is necessary to increase the size of the wires to reduce the resistivity. Furthermore, large rails decrease the resistive heating, which leads to longer rail life.

An effective way to limit the damaging effects of high electrical current in the firing circuit is to prevent the current from reaching damaging levels. This is done by inserting a resistor in the firing circuit of the railgun. This reduces current in accordance with Ohm’s Law, which says that current is inversely proportional to resistance in a resistor circuit. However, this also reduces the magnetic field which will reduce the acceleration, and as such has not been included in my design.

Another aspect of current flow within the firing circuit is the discharge time. In an ideal railgun, the discharge time would be zero, so that the maximum force is exerted in the minimum amount of time. Unfortunately, this is impossible in the real world, and so we must address this aspect. If we assume that the capacitance (and therefore the total potential energy of the system) is fixed, then it is safe to assume that as the discharge time increases, the maximum

current developed in the firing circuit decreases. This decreases wear and tear on the railgun, but also decreases the impulse on the projectile. Thus, it is important to strike a balance between high current and long component life.

A notable detail of the current during firing is that it is not constant for the duration of the capacitor discharge. When capacitors are discharged (or charged), the current depends exponentially on time. Maximum current occurs just after the switch is closed, then decrease exponentially as the capacitors drain. For the resistance and capacitance values of this circuit, the discharge can be assumed to be instantaneous.

Friction is another variable which must be recognized in the design of railguns. A projectile and rail combination must be designed such that contact between the projectile and the rails is maximized while minimizing friction. Maximizing the contact area minimizes local heating while maximizing current (and increasing friction), but minimizing friction maximizes acceleration. These two requirements seem to contradict each other, and so a compromise must be found. Preliminary research yielded a design which used square rails. I decided to use round rails because they seemed to be the best compromise between friction and contact area when combined with a spherical projectile.

Safety Issues

One would expect a device such as this, which involves high voltages, large currents, and large amounts of stored energy, to be fairly dangerous, and one would be correct. The rails themselves are dangerous, because they are completely exposed during firing and can be triggered by anything metallic contacting both rails at the same time. I constructed a wooden cover for the rails for when the capacitors are charging (as there is no switch in the firing circuit due to resistance concerns, it is armed at all times), so that inadvertent contact with the rails was impossible. The other main source of danger is the contacts on the tops of the capacitors.

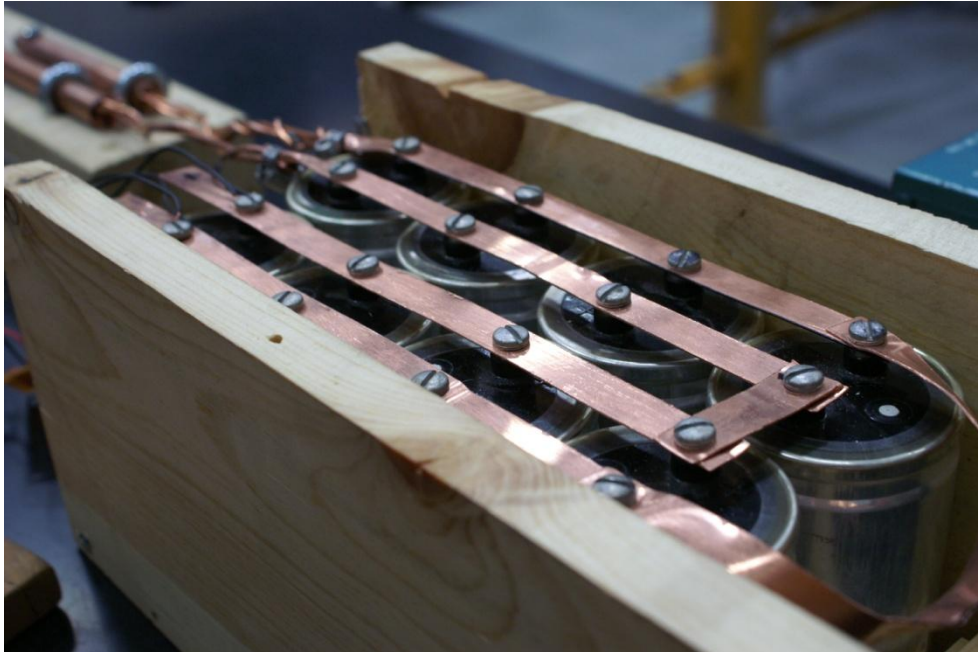


Figure 4: Pictured is the capacitor bank, with the copper strips which form the electrical connection visible. Contact with these strips when the capacitors is a significant safety risk.

These carry the same current as the rails, and are discharged by firing the device. They are electrically connected to each other with flat, bare strips of copper. This necessitates another wooden cover for the tops, which I fastened to the box which houses the capacitors. With these two safety features in place, the final electrical danger is the charging circuit. Currently, it is unprotected, but it could easily be housed in a container.

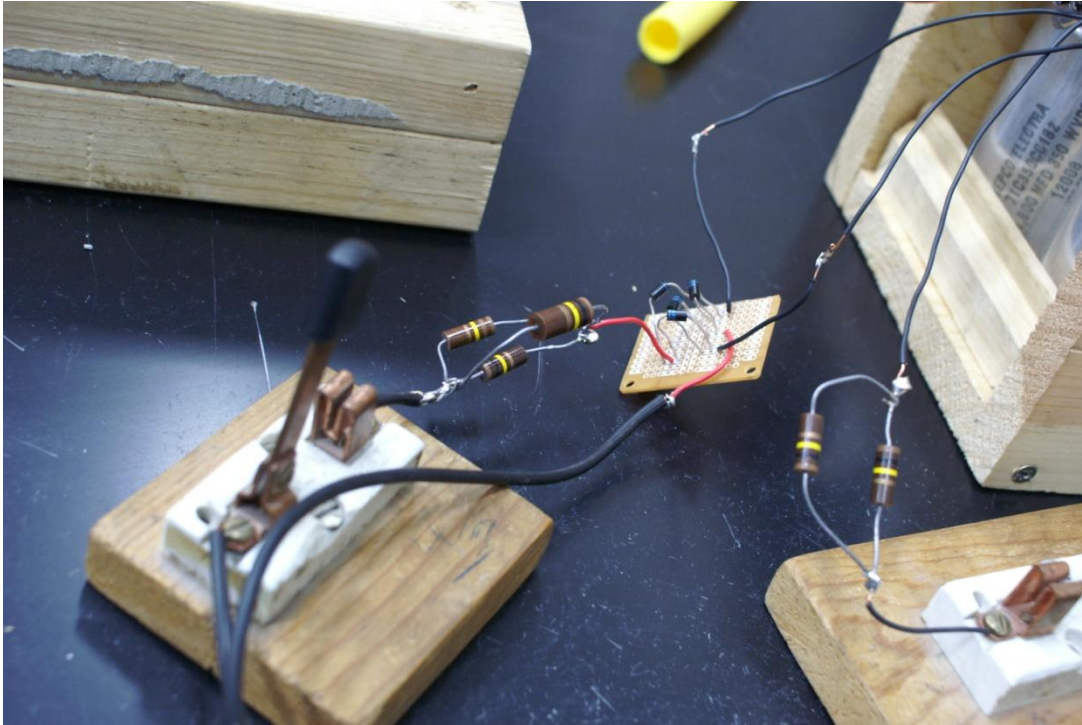


Figure 5: The exposed charging circuit, illustrating the potential danger of this component. All visible electrical connections carry charging voltage, which is generally between 10 and 120 volts.

The last and most obvious danger is posed by the purpose of building the device in the first place: the flying projectile. This danger can be mitigated if the user follows basic firearms safety rules. If the user practices common sense this device is, overall, relatively safe.

Model Results

To verify the model, firing was necessary. For safety, we decided to charge the capacitor bank to 25 volts and fire it. Assuming all went well, we would then charge it to 60 volts, and fire again.

During testing, I measured charging times to be about 22 minutes to reach 25V potential across the capacitors, with a charging AC voltage of 140 V. I did not record exactly how long it took to reach 60 volts, but it is approximately 45 minutes.

The railgun did function, in that a large current was passed when a piece of lead shot was placed between the rails, accompanied by bright flashes which were reminiscent of arc welding.

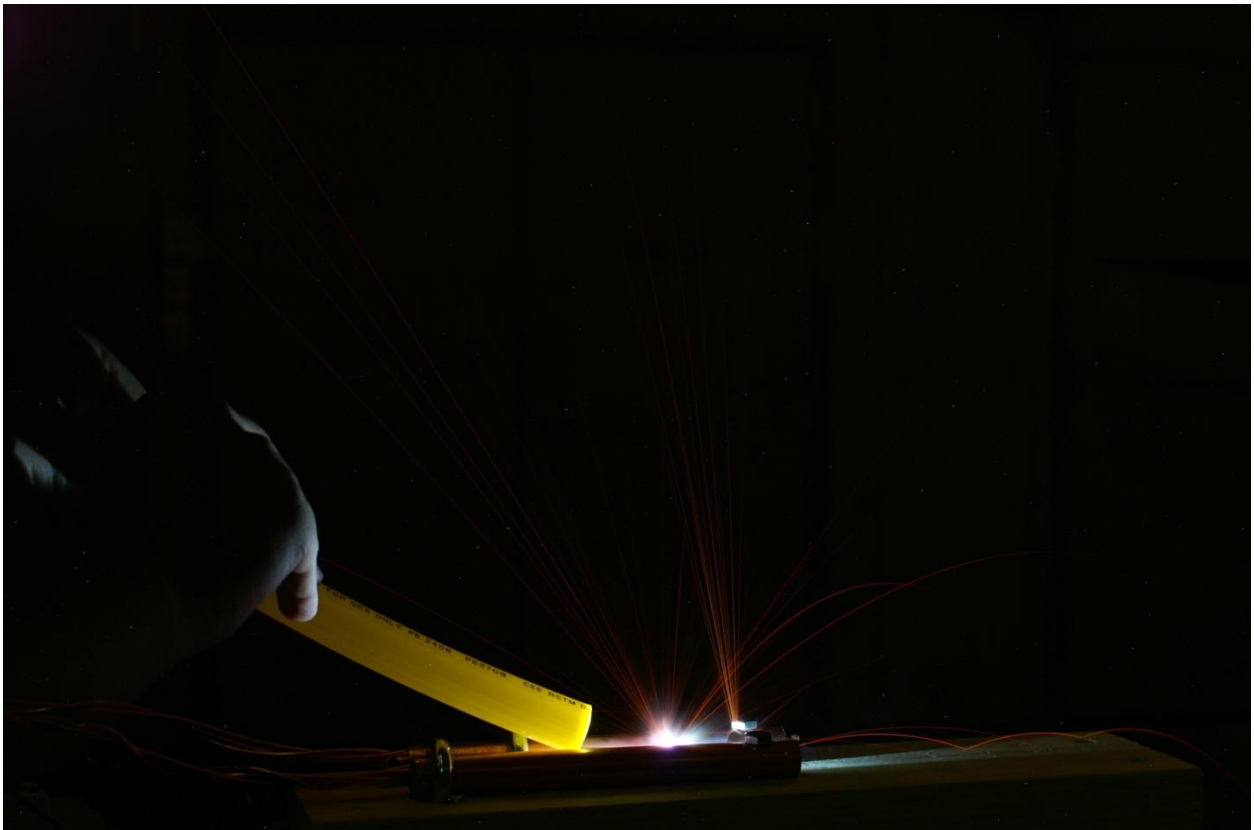


Figure 6: Long exposure of railgun test-fire at 60 volts. The orange, arcing streak is the trajectory of the ball. Note the tube used to impart initial velocity to the ball in order to prevent sticking.

This flash was present at both voltages, but was far more pronounced and dramatic at 60 volts. However, I was never able to produce any forward acceleration using the railgun. It is possible that the current was not high enough (the capacitors were only ever charged to a maximum of 60 volts due to equipment shortfalls, rather than the device maximum of 350 volts). I used Ohm's Law to estimate the peak current to be in the neighborhood of 12 amps. Neglecting imperfections in the magnetic field and the device, this current should produce a total force of $9 \cdot 10^{-6}$ Newtons. Using the previous example of the .45 caliber, 133 grain lead ball, the final theoretical final velocity would be in the neighborhood of 78 m/s, which is approximately 256 ft/s. This calculation can be seen in Appendix C. This is the generally-accepted maximum muzzle velocity of a standard paintball gun (EMR Paintball).

I determined that a likely cause of the lack of movement was the magnetic field being weaker than expected due to the uneven packing of the wire inside of the pipes, which left pockets of air throughout the rails.

Data Analysis

After constructing the first railgun design and determining that it does not (noticeably) work, I collected magnetic field data from a single rail using a constant-current power source. The experimental set up consisted of the rail assembly detached from the remainder of the railgun, so that the rails were electrically isolated. I then attached leads from a high-current power source to one of the rails, and applied a potential which created a current ranging between 8.67 and 8.81 amperes. Then, using a magnetometer and a Texas Instruments CBL system, I measured the magnetic field along the length of the rod every half-inch, 1 mm away from the rod.

The resulting data of the normalized magnetic field vs. distance along the rod can then be graphed and is seen in the following figure, Fig. 7.

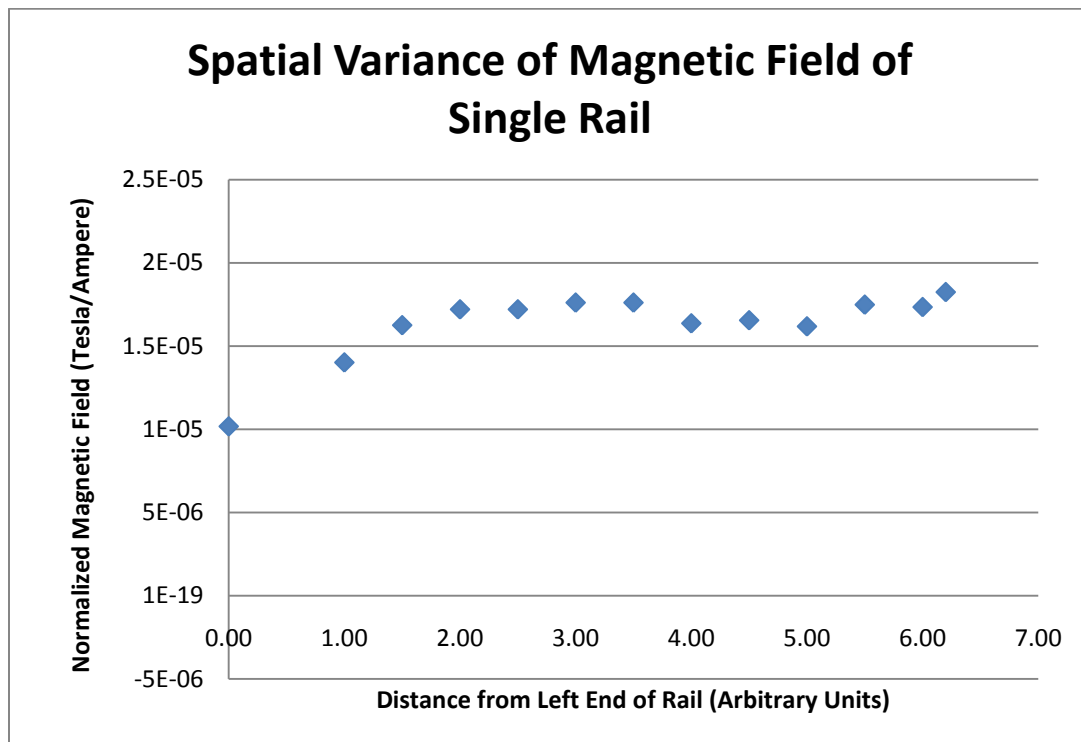


Figure 7: Distance from left end of rail vs. current-normalized magnetic field. The second data point is missing due to construction limitations.

The resulting figure is striking: a smooth, concave down curve ending at the center of the rod, at which point the curve switches to be concave up. This uneven magnetic field data indicates that the magnetic field itself varies widely along the length of the rod in places where, theoretically, it should not. The curve should be steady and concave down over the length of the rod, reflecting a maximum magnetic field in the center of the rod (where the rod approximates an infinitely long wire) and minimum fields at either end. The graph is not symmetric, but from a practical view, that is not important. Depending on railgun design, it is possible that this relatively-steady field would be desirable.

The data has a maximum field of 1.58 Gauss, located at the right end of the rod. The minimum field was measured at the left end, having a value of 0.90 Gauss. This variance is expected, but the location of the maximum is indicative of the uneven nature of the field from the void-filled rod.

The current supplied by the power supply slowly decreased during the course of the test. As a result, the output current slowly decreased. This should decrease the measured magnetic field (especially near the right end of the rod), but the measurements contradict this. Therefore, the magnitude of the error caused by this drop in current is small compared to the unevenness of the field.

I believe that the unevenness of the field is due to voids throughout the rod due to the construction method. Therefore, the next set of data was from a solid wire. The set up was the same as before, but instead of the wire-filled rod, I used a single strand of copper wire which I straightened to the best of my abilities. The current ranged from 8.45 to 8.52 amperes. I measured the field from the wire in the same fashion as before.

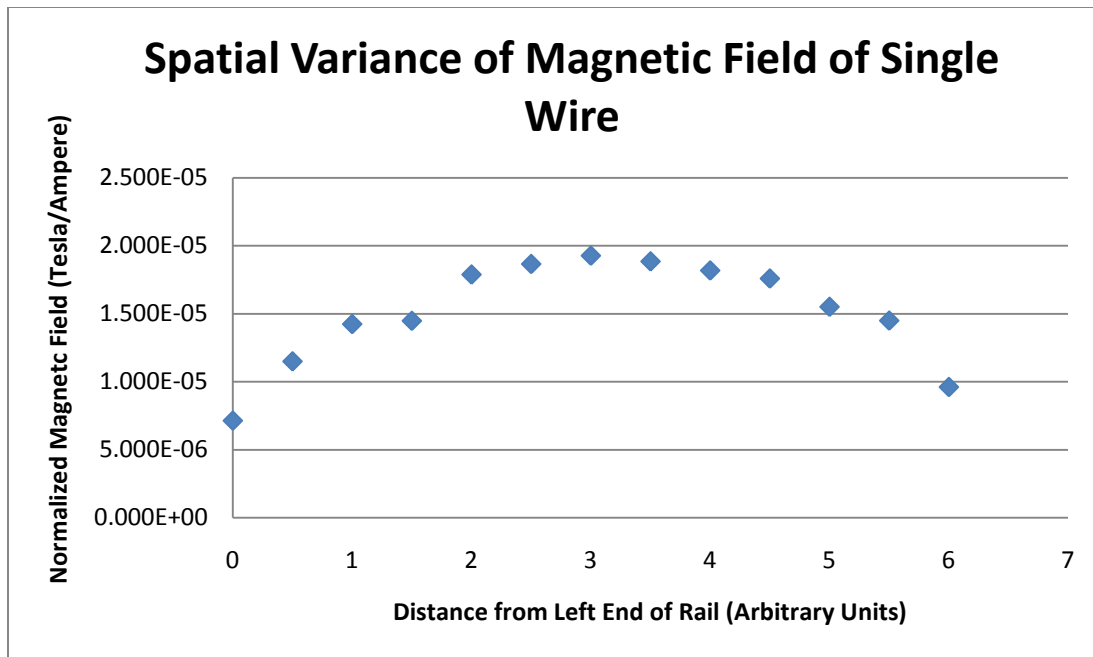


Figure 8: Distance from left end of rail vs. current-normalized magnetic field. Note the smooth curve, which is expected for this experiment.

The resulting data looks as expected: a consistent concave-down curve with a maximum field at the middle of the wire, and minima at either end. This is consistent with the expected result, and shows that a solid wire can produce a symmetric magnetic field around a peak value. This result suggests that to improve the current railgun design, I should replace the wire-filled rods with machined solid bars to eliminate voids to reduce magnetic field inconsistencies.

Consequent Investigation

The previous magnetic field measurement experiments were helpful in determining the shape of the magnetic field. However, having no accurate way of calibrating the measurement equipment meant that the data generated could not be trusted in terms of exact magnetic field measurements. To verify the magnetic field measurements, I decided to develop a numerical model of the copper wires. This would help to determine the correct magnitude of the magnetic field, as well as verify the shape of the field as a function of distance along the rod.

Equation One is for the average magnetic field between two long straight wires. I measured the magnetic field due to a single wire, and so I used Equation Five, below.

$$B = \int \frac{\mu_0 I d\vec{L} \times \vec{r}}{4\pi |r|^3} \quad \text{Eq. 5}$$

This equation was integrated numerically. The wire was divided into n user-specified intervals.

The vector cross-product was evaluated for each interval of the wire. Equation Five then becomes:

$$B \approx \frac{\mu_0 I}{4\pi} \sum_{i=0}^n \frac{dl \cdot y}{|r|^3} \quad \text{Eq. 6}$$

in this equation, n is the number of user-specified intervals, y is the radial distance from the centre of the wire, and r is the Euclidean distance from dl distance to the test point. This is shown in Figure 8.

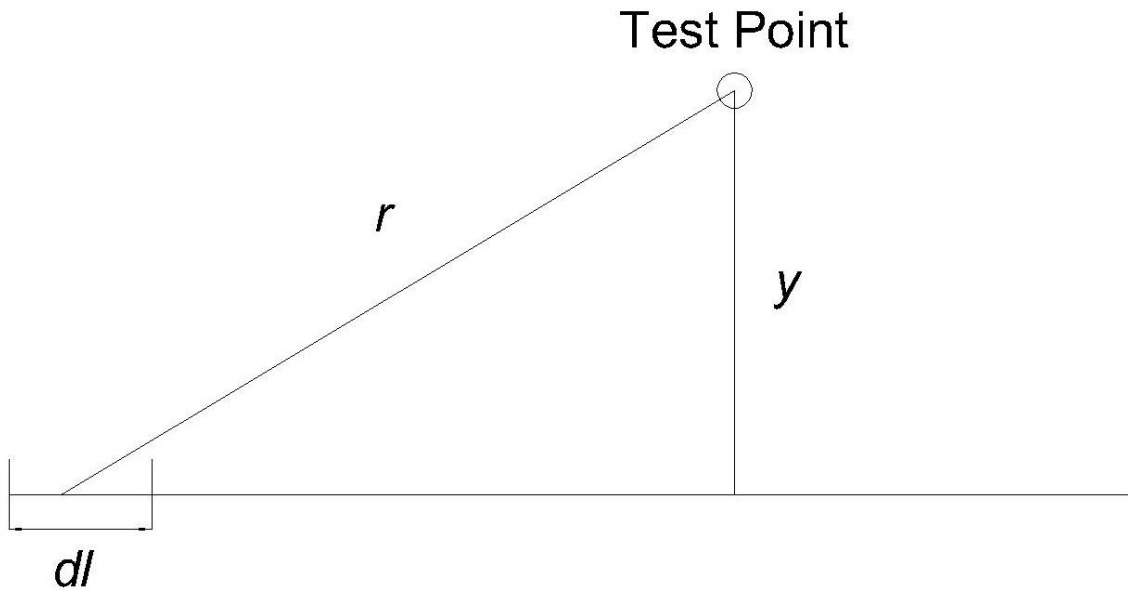


Figure 9: Numerical method for calculating magnetic field from a finite wire.

I implemented this in a MATLAB program, which sums the total magnetic field at points along the entire length of the wire. This produces a graph with the same data as the field measurement graphs.

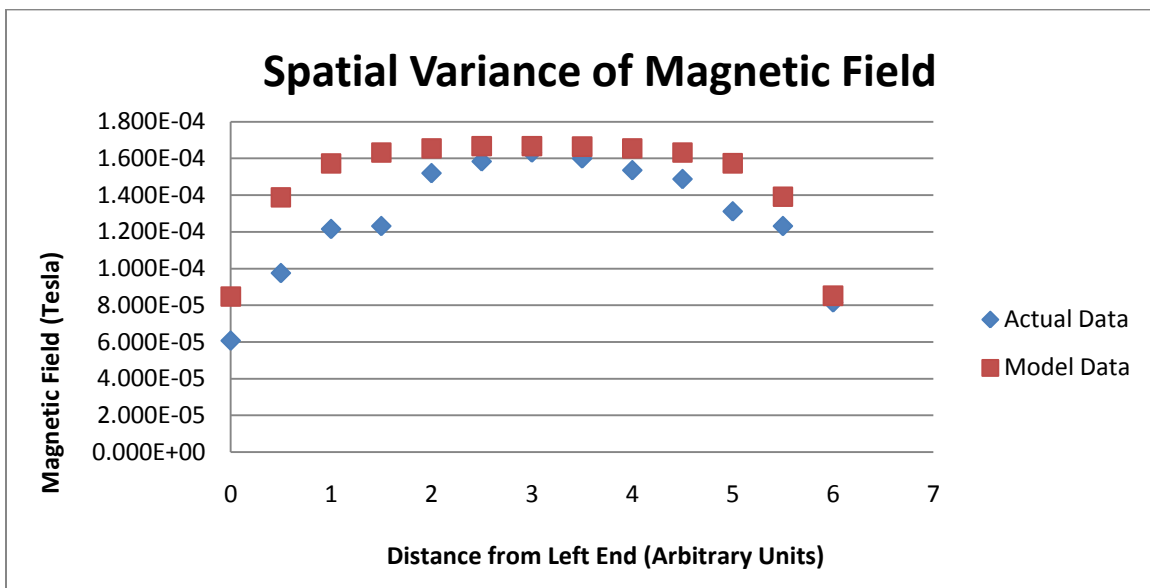


Figure 10: Numerical approximation of magnetic field data in red, with actual data plotted in blue. This data replicates that of the single wire measurement experiment.

This graph has a slightly different shape as the empirical data. However, the central value, which is the maximum, is 1.67×10^{-4} Tesla, compared to 1.63×10^{-4} Tesla that was measured experimentally. This is a difference of 2.10%. I then compared the numerical result to that of an infinitely long, straight wire. This figure is 1.700×10^{-4} Tesla, which has an error of 1.94% when compared to the numerical result, or 4% when compared to the empirical data. This is an acceptable error in both cases, and can be attributed to numerical approximation error, measurement error, and the fact that the wire is not of infinite length as required by Ampere's Law. However, the error increases as we move to the left or right of the center.

The table in appendix A shows measurements at half-inch intervals along the length of the wire, along with the numerical model's approximation and the long, straight wire result (provided by Ampere's Law). The smallest error is at the center of the wire. This is expected, especially for Ampere's Law. Therefore, the center of the wire will be the closest approximation of an infinitely long wire. The error between Ampere's Law and the measurement grows very quickly as the test point moves away from the center of the wire. This is also true of the model error when compared to the measured field, but the increase is not nearly as drastic. The maximum error is about a third of that of Ampere's Law. This shows that the numerical model is better at approximating the wire than Ampere's Law.

The error between measurements and the approximation likely stems from a combination of human error, equipment error, and numerical integration error. This error could be reduced through more careful measurement, more accurate measurement devices, and more accurate numerical modeling methods.

Conclusion and Future Work

Railguns present a fascinating and challenging design problem. Over the course of this project, I designed and built a model railgun, then wrote a MATLAB program to model the behavior of the rails during firing. This numerical model is an important design tool, since it offers insight into the behavior of the magnetic field, which can't be seen. The physical model helped me to determine problems that the numerical model could not: local heating due to current flow, and the difficulties of actually building the device. They are the ultimate modern-day projectile launching device, but making them more powerful has the capacity to destroy them.

I have many ideas of how to improve my current railgun design. The first is to replace the current rails with solid copper bars, to facilitate a stronger magnetic field. I would also like to replace the projectile. Lead does not seem to be an ideal material, due to its very low melting point and malleability. A better projectile would be aluminum or copper; aluminum due to its low density and high conductivity, and copper due to its very high conductivity. I would also like to try tungsten, because its extremely high melting point would resist welding caused by local heating, and its high density would enable a very small projectile to be used. The launch method could also be improved. I would like to build a device similar to the one MIT used to great success. With these three main improvements, I believe the railgun would function much more effectively.

Appendix A

| Measured B field (Tesla) | Model Field Approximation | Model Error | Long Straight Wire | Long Straight Wire vs Measurement Error |
|--------------------------|---------------------------|-------------|--------------------|---|
| 6.080E-05 | 8.48E-05 | -28.2858 | 1.70E-04 | 64.2353 |
| 9.760E-05 | 1.39E-04 | -29.6931 | 1.70E-04 | 42.5882 |
| 1.216E-04 | 1.57E-04 | -22.6709 | 1.70E-04 | 28.4706 |
| 1.232E-04 | 1.63E-04 | -24.4959 | 1.70E-04 | 27.5294 |
| 1.520E-04 | 1.65E-04 | -8.1404 | 1.70E-04 | 10.5882 |
| 1.584E-04 | 1.67E-04 | -4.9465 | 1.70E-04 | 6.8235 |
| 1.632E-04 | 1.67E-04 | -2.0996 | 1.70E-04 | 4.0000 |
| 1.600E-04 | 1.66E-04 | -3.8693 | 1.70E-04 | 5.8824 |
| 1.536E-04 | 1.65E-04 | -7.1847 | 1.70E-04 | 9.6471 |
| 1.488E-04 | 1.63E-04 | -8.8291 | 1.70E-04 | 12.4706 |
| 1.312E-04 | 1.57E-04 | -16.6243 | 1.70E-04 | 22.8235 |
| 1.232E-04 | 1.39E-04 | -11.4879 | 1.70E-04 | 27.5294 |
| 8.160E-05 | 8.52E-05 | -4.2085 | 1.70E-04 | 52.0000 |

Figure 11: A comparison of magnetic field measurement, numerical approximation, and Ampere's Law. The numerical model is at least 60% better than Ampere's law at approximating the measured data.

Appendix B

MATLAB Numerical Program

```

clear all
clear figure

mu=4*pi()*10^-7; %Vacuum permeability
i=0;
I=8.5; %current in amps
k=1;
y=.01; %y distance of point vertically from wire
xPrime=0;
n=2000; %number of intervals along the wire - relatively small error if
l is a factor of n or vice versa
l=.1; %length of wire in meters
dl=l/n;
rAmpere=y;
B=zeros(n,1); %preallocate matrix, units are Teslas (SI unit)

% summation
for x=0:dl:l;
    sum=0;
    xPrime=0;
    for i=0:n;
        r=sqrt((x-xPrime)^2+y^2);
        xPrime=xPrime+dl;
        sum=sum+(dl*y)/(abs(r)^3);
    end

    B(k)=(mu*I)/(4*pi())*sum;
    k=k+1;

end

plot(B);
ylim([0,B(n/2)]);
xlim([0,n]);
xlabel('n (multiply by "dl" to yield distance in meters)')
ylabel('Tesla')
title('Plot of Magentic Field vs Distance from Left End of Wire')

% Ampere's Law
BAmpere=(mu*I)/(2*pi()*rAmpere)

B=B(1)

```

Appendix C

Calculation of Theoretical Final Velocity

The electrical energy stored in the capacitors is potential energy, so we write:

$$\text{PE} = \text{Electrical potential energy}$$

PE can be transformed into KE easily (such as dropping an object), we can assume that all of the potential energy from the capacitors is converted into kinetic energy.

$$\text{KE} = \text{PE}$$

The kinetic energy formula:

$$\text{KE} = \frac{1}{2}mv^2$$

Where m is the mass of the projectile, v is the theoretical final velocity, and KE is the kinetic energy of the object.

Thus, we can calculate the final velocity of the object by combining the two previous equations.

$$\text{PE} = \frac{1}{2}mv^2$$

Thus, if we know the stored energy in the capacitors, we know the theoretical final velocity of an object fired by the railgun.

Works Cited

EMR Paintball. (n.d.). *Paintball Info*. Retrieved April 2011, from EMR Paintball Park: <http://www.emrpaintball.com/info.shtml>

Fauchon-Villeplee, A. L. (1922). *US Patent 1,421,435 "Electric Apparatus for Propelling Projectiles"*.

Harris, W. (2005, October 11). *How Rail Guns Work*. Retrieved March 2011, from <http://science.howstuffworks.com/rail-gun1.htm>

Hogg, I. V. (1969). *The Guns: 1939/45*. Macdonald.

Horowitz, H. (1980). *The Art of Electronics*. Cambridge: Cambridge University Press.

Knight, R. D. (2004). *Physics for Scientists and Engineers*. San Francisco: Pearson-Addison Wesley.

NavWeaps. (2009, November 22). *United States of America - 16"/50 (40.6 cm) Mark 7*. Retrieved April 2011, from NavWeaps: http://www.navweaps.com/Weapons/WNUS_16-50_mk7.htm

Walter, J. (1999). *A Tabletop Demonstration Railgun*. Retrieved October 2010, from <http://web.mit.edu/mouser/www/railgun/halluc/intro.html>